energies

MDPI

Review

Recent Advancements in Pd-Based Membranes for Hydrogen Separation

Nadia Cerone [1], Giuseppe Domenico Zito [2], Carmine Florio [1], Laura Fabbiano [2] and Francesco Zimbardi [1,*]

[1] Energy Technologies and Renewable Sources Department, ENEA, ss Ionica 106, 75026 Rotondella, Italy; nadia.cerone@enea.it (N.C.); carmine.florio@enea.it (C.F.)
[2] Department of Mechanics, Mathematics and Management, Polytechnic University of Bari, Via Orabona 4, 70125 Bari, Italy; g.zito5@phd.poliba.it (G.D.Z.); laura.fabbiano@poliba.it (L.F.)
* Correspondence: francesco.zimbardi@enea.it; Tel.: +39-0835-974-310

Abstract: The use of hydrogen is pivotal for the energy and industrial transition in order to mitigate the effects of climate change. As technologies like fuel cells, e-fuels, and the semiconductor industry increasingly demand pure hydrogen, the development of efficient separation methods is crucial. While traditional methods such as pressure-swing adsorption are common, palladium (Pd)-based membranes are a promising alternative due to their energetic efficiency. This review summarizes the recent advances in Pd-based membranes for hydrogen separation over the last six years. It provides a theoretical overview of hydrogen permeation through membranes and examine the characteristics of various Pd alloys adopted in membrane fabrication, discussing the advantages and disadvantages of binary and ternary alloys, for different membrane types, including self-supported and supported membranes, as well as the role of intermediate layers. Additionally, the membrane characteristics used in some recent works on self-supported and supported Pd membranes are analyzed, focusing on operational parameters like permeability, selectivity, and durability. Finally, this review emphasizes the significant progress made in enhancing membrane performance and discusses future directions for industrial applications.

Keywords: hydrogen; separation; membrane; palladium; Pd-based membranes

Citation: Cerone, N.; Zito, G.D.; Florio, C.; Fabbiano, L.; Zimbardi, F. Recent Advancements in Pd-Based Membranes for Hydrogen Separation. *Energies* **2024**, *17*, 4095. https://doi.org/10.3390/en17164095

Academic Editor: Vladislav A. Sadykov

Received: 28 June 2024
Revised: 25 July 2024
Accepted: 26 July 2024
Published: 17 August 2024

1. Introduction

One of the major challenges our society is facing today is represented by the effects of climate change. According to the World Meteorological Organization (WMO), the mean temperature on the Earth's surface has reached a new record increase of +1.45 °C above pre-industrial levels [1]. In this scenario, where the limit of 1.5 °C set during COP26 is close to being reached, the target is to mitigate global warming effects. Increasing decarbonization and reducing greenhouse gas (GHG) emissions are the first steps towards this goal. Hydrogen plays a key role in the energy transition because its combustion or oxidation does not emit GHG. In addition, it can be produced by renewable sources, completely avoiding these emissions [2]. Depending on the production process, hydrogen can be categorized into different colors:

- Brown or black: produced by coal (lignite or bituminous coal) gasification;
- Grey: produced via steam reforming of methane;
- Blue: produced via steam reforming or gasification but with the adoption of Carbon Capture Utilization and Storage (CCUS) technologies;
- Turquoise: produced via methane pyrolisis;
- Yellow: produced via electrolysis using the electricity from the grid;
- Pink or red: produced via electrolysis or thermo-catalysis through the energy (electrical or thermal) derived from nuclear plants;
- Orange: produced by biomass [3];

- Green: produced using renewable sources [4].

Currently, hydrogen is mostly produced from fossil fuels, but novel production methods involving recycling, for example, of waste plastics [5], are being actively investigated. Approximately 62% of global hydrogen is produced from natural gas, with or without CCUS, and 21% from coal, with only 0.1% derived from electrolysis [6]. The International Energy Agency reported a growing use of hydrogen predominantly within traditional sectors, including the refinery and chemical industry. However, hydrogen adoption in other sectors like heavy industry (hard-to-abate sectors) and transport is increasing [6]. In the transport industry, besides recent research on hydrogen storage [7–9], pure hydrogen is required for the adoption of Proton Exchange Membrane Fuel Cells (PEMFCs) which are highly sensitive to carbon monoxide poisoning [10]. Hydrogen produced via electrolysis is not widely used for this purpose, because the hydrogen adopted in fuel cells needs to be particularly pure following the requirements stated in the ISO 14687:2019 [11]. There are several physical and chemical methods used for hydrogen purification [12]. Among the physical methods, the ones that guarantee the highest hydrogen purity are Pressure Swing Adsorption (PSA) [13] and membrane separation, in particular with dense metal membranes [14]. Various studies have been conducted on dense metal membranes, particularly for palladium-based (Pd) membranes, which represent the most widespread and investigated types. In the last six years, several reviews on membranes for hydrogen separation have been published. The most comprehensive ones include a summary of modern hydrogen production technologies involving membranes and membrane reactors [15–18]; a review on the state of the art on the Water–Gas Shift reaction including membrane reactors [19]; the performances of Pd-based membranes [20–22]; and the applications of Pd-based membranes for low-pressure hydrogen isotopes in nuclear fusion [23]. The development of Pd-based membranes is an active topic in the scientific community according to the number of papers published in the last six years, with a peak in the number of articles in 2020, as shown in Figure 1 and in Tables 1 and 2 (Scopus database). This review provides an overview of the state of the art of Pd-based membranes and the significant progress and direction taken by researchers in the last few years.

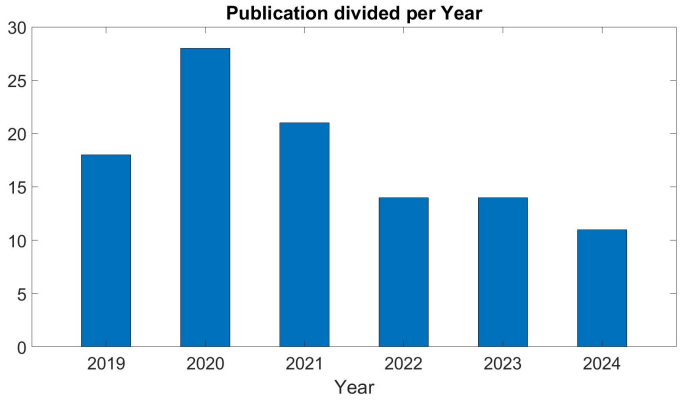

Figure 1. Publications on Pd-based membranes for hydrogen separation in last 6 years.

Table 1. Publications on Pd-based membranes for hydrogen separation in last 6 years.

Year	Number of Publications
2024	11
2023	14
2022	14
2021	21
2020	28
2019	18

Table 2. Major investigators of Pd-based membranes for hydrogen separation in the last 6 years.

Researcher	Number of Publications
Gallucci, F.	11
Sanz, R.	7
Calles, J. A.	7
Alique, D.	7
Martinez-Diaz, D.	5
Chen, W. H.	5

2. Hydrogen Permeation through Membranes

Membranes are defined as selective barriers that allow some substances to pass through while blocking others. Hydrogen permeation through selective membranes has been extensively studied. An overview of membranes used for hydrogen purification is provided in Figure 2. There are four major types of membranes: inorganic, metallic, polymeric, and proton-conducting membranes. Inorganic membranes can be divided into mesoporous and microporous membranes, depending on the porous dimension; for example, zeolites belong to micro-porous membranes. Proton-conducting membranes are divided into dense ceramic membranes, which include perovskites, and cermet membranes. Dense metallic membranes include Pd-based membranes, which are the most used ones due to the specific characteristics of Pd. Palladium (Pd), which was discovered in 1803 by William Hyde Wollaston, has the capacity of dissociating hydrogen gas into its mono-atomic form, absorbing about 600 times its volume in hydrogen [24]. This is due to its electronic configuration $1s^2$ $2s^2$ $3s^2$ $4s^2$ $3d^{10}$ $4p^6$ $4d^{10}$ $5s^0$; the overlapping energy bands between the 4d and 5s orbitals of Pd confer the property of accepting donor electrons from other atoms [25]. Hydrogen permeation happens in seven steps, as illustrated in Figure 3:

1. Diffusion of molecular hydrogen through the surface of the membrane;
2. Dissociation of molecular hydrogen on the palladium surface;
3. Dissolution of atomic hydrogen into the bulk metal;
4. Diffusion of atomic hydrogen through the bulk metal;
5. Association of atomic hydrogen on the palladium surface;
6. Desorption of molecular hydrogen from the surface;
7. Diffusion of molecular hydrogen from the surface [26].

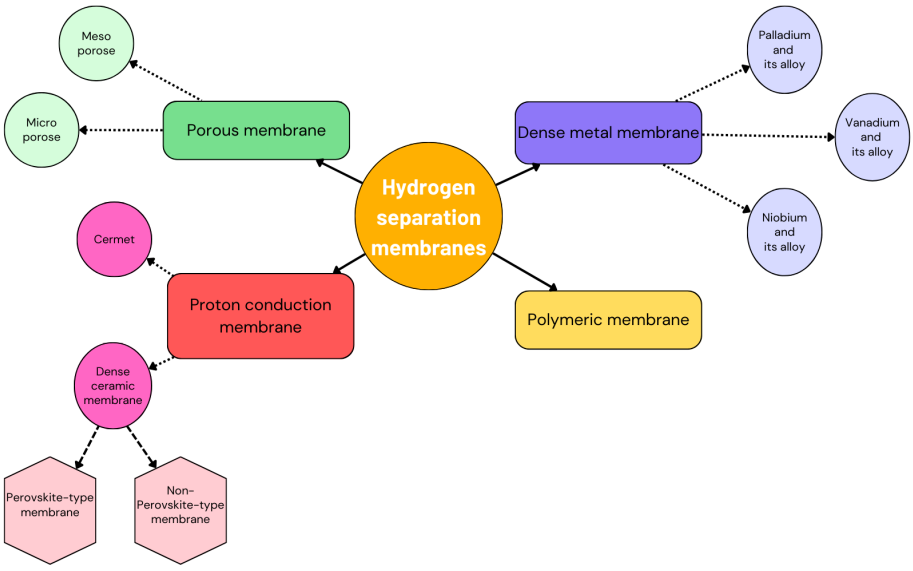

Figure 2. Types of membranes used for hydrogen separation.

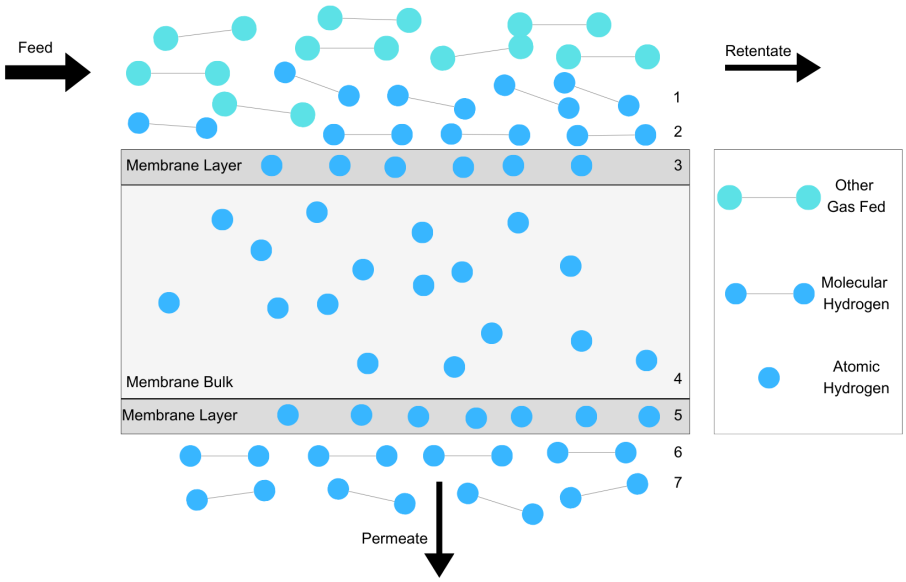

Figure 3. Adsorption–desorption mechanism in Pd-based membranes, adapted from [27].

The permeation of hydrogen (H_2) through a metallic membrane follows the steady-state diffusion mechanism of a gas into a metal, modelled by Fick's law in Equation (1):

$$J = -D\frac{\partial C}{\partial x} \tag{1}$$

where J is the diffused flux, D is the diffusion coefficient, and $\partial C/\partial x$ is the concentration gradient. In gas diffusion, both concentration and pressure gradient participate. For gases, the relationship between concentration and pressure is a constant set by Henry's law in Equation (2):

$$S_H = \frac{C_{gas}}{P_{gas}} \tag{2}$$

where S is a constant defined as the ratio of the non-dissociative gas concentration in a solid or liquid at dilute concentration C_{gas} to its vapor pressure P_{gas}. Typically, obtaining information on the concentration gradient is challenging, and Fick's law (Equation (1)) is rearranged using Henry's law (Equation (2). The constant S_H is also referred to as the solubility S and it is measured as a concentration per unit of pressure. The H_2 molecule is dissociated in the atomic form before permeation through the membrane, and the German chemist Adolf Sieverts refined Henry's law, demonstrating that for diatomic gases, such as H_2, the solubility is a function of the square root of the pressure:

$$S_H = \frac{C_{H_2}}{P_{H_2}^{1/2}} \tag{3}$$

Equation (3) is called Sieverts' law. Substituting Sieverts' law in Equation (1) and rearranging:

$$J_{H_2} = D \cdot S \cdot \frac{\partial P_{H_2}^{1/2}}{\partial x} \cong D \cdot S \cdot \frac{\Delta P_{H_2}^{1/2}}{\Delta x} \tag{4}$$

where Δx is the membrane thickness, which can be approximated by x. The H_2 flux is expressed in mol$\cdot$ m$^{-2}\cdot$ s^{-1} and (Equation (4)) can be rearranged to obtain the moles that go through the membrane, multiplying with the active membrane surface (A) and the time (t)

$$Q = J \cdot A \cdot t = D \cdot S \cdot \frac{A}{x} \cdot \Delta P_{H_2}^{1/2} \cdot t \tag{5}$$

The product between the diffusivity and the solubility is the permeability K defined as the property of a gas to diffuse through a solid material. Differentiating the moles with respect to time, an expression for molar flow is obtained in Equation (6):

$$\dot{Q} = K \cdot \frac{A}{x} \cdot \Delta P_{H_2}^{1/2} \tag{6}$$

The definition of the permeability K leads to a simplified expression for the H_2 flux is reported in Equation (7)

$$J_{H_2} = K \cdot \frac{(P_1^n - P_2^n)}{x} \tag{7}$$

where P_1^n is the H_2 partial pressure on the feed side, P_2^n is the H_2 pressure on the permeate side, and n is the coefficient for the diffusion mechanism that can vary between 0.5 and 1, depending on the type of membrane (metallic or porous). Both solubility S and diffusivity D follow an Arrhenius-type relation, and so does the permeability. These relations are reported in Equations (8)–(10):

$$S = S_0 \cdot e^{\frac{-E_S}{R \cdot T}} \tag{8}$$

$$D = D_0 \cdot e^{\frac{-E_D}{R \cdot T}} \tag{9}$$

$$K = K_0 \cdot e^{\frac{-E_K}{R \cdot T}} \tag{10}$$

where E_S, E_D,E_K are the activation energies. The three activation energies are linked by Equation (11):

$$E_K = E_S + E_D \tag{11}$$

To normalize the permeability, typically, the permeance is reported, defined as the ratio between permeability and membrane thickness (Equation (12)):

$$K_x = \frac{K}{x} \rightarrow J = K_x \cdot (P_1^n - P_2^n) \tag{12}$$

Another important parameter is selectivity, which is defined as the membrane's ability to allow one specific gas to diffuse through while restricting others. This is typically estimated by evaluating a gas mixture containing two elements (A and B) using Equation (13):

$$\alpha = \frac{(y_A / y_B)_{permeate}}{(y_A / y_B)_{feed}} \tag{13}$$

Two other important parameters adopted to evaluate the performance of membranes are based on molar ratios:

- recovery S_r defined as the ratio between permeated and feed gases, reported in Equation (14):

$$S_r = \frac{q_p}{q_f} \tag{14}$$

  where q_p is the permeate flow and q_f is the feed flow.
- volume reduction VR, defined as the ratio between feed and retentate flow, reported in Equation (15):

$$VR = \frac{q_f}{q_r} \tag{15}$$

3. Characteristics of Palladium and Its Alloy Membranes

Dense membranes are characterized by the highest hydrogen permeability at a wide range of temperatures. The metals that exhibit the highest hydrogen permeability include niobium, vanadium, tantalium, and palladium. The first three metals provide hydrogen permeabilities in the order of 10^{-7} and 10^{-5} mol· m^{-1}· s^{-1}· $Pa^{-0.5}$ [28]. However, their hydrogen permeability is effective only between 350 °C and 650 °C, as they

are susceptible to significant hydrogen embrittlement due to their Body-Centered Cubic (BCC) structure [29]. Palladium, on the other hand, provides lower hydrogen permeability (around 10^{-8} mol· m^{-1}· s^{-1}· $Pa^{-0.5}$) but at a wider temperature range [28], due to its Face-Centered Cubic (FCC) structure, which makes this metal more resistant to hydrogen embrittlement [29]. However, at the temperature of 295 °C, called critical temperature (T_c), there is the coexistence of two phases: an interstitial solid solution (α) and a Pd hybrid phase (β). Both have the FCC structure but different lattice parameters, and their coexistence occurs in a lattice volume expansion of 10% that generates internal stresses, which can lead to membrane failure after repeated sorption and desorption cycles [30]. Another drawback of using palladium membranes is poisoning by other molecules such as carbonaceous species, carbon monoxide and propene, and hydrogen sulfide. Carbon monoxide interferes with Pd active sites, blocking hydrogen adsorption in these sites [31]. Propene poisoning, on the other hand, involves the decomposition of the molecule on the membrane surface into species that modify the electronic structure of Pd, reducing its ability to dissociate molecular hydrogen in atomic form [31]. The carbon monoxide poisoning effect decreases with temperature, while propene poisoning increases with temperature [31]. Hydrogen sulfide poisoning involves two steps:

1. Adsorption on the Pd-based membrane surface;
2. Dissociation of hydrogen sulfide:

$$H_2S \rightarrow H^+ + SH^-$$

$$SH^- \rightarrow H^+ + S^{2-}$$

The sulfur ion adsorbed in Pd bulk is bound into the FCC structure and blocks hydrogen adsorption in the contiguous sites [32]. Furthermore, the increasing cost of palladium over the years drove the research towards exploring palladium alloys to overcome these limitations. The palladium price in the last 16 years is reported in Figure 4.

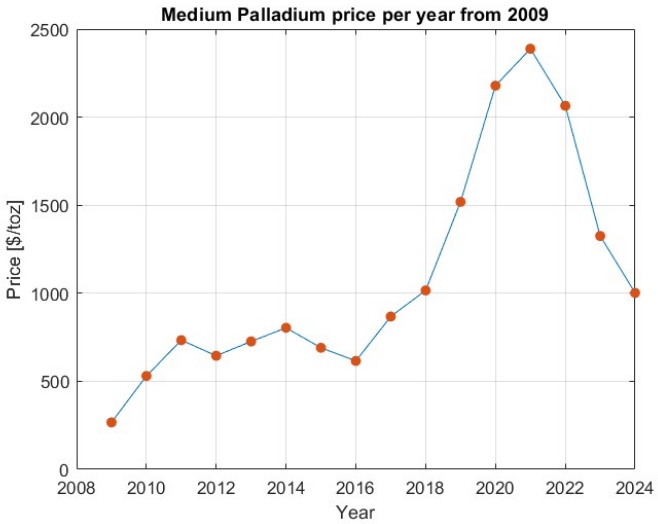

Figure 4. Palladium price over last 16 years [USD/toz] [33].

3.1. Palladium Alloys Adopted in Membrane Fabrication

The most investigated and commercially adopted Pd alloy is the silver alloy with Ag content between 20% and 25%. The Pd-Ag alloy is less expensive than pure Pd, can be used at lower temperatures due to lower T_c (around room temperature), and provides higher permeability values than pure Pd; on the other hand, Pd-Ag alloys are more sensitive to CO poisoning than pure Pd because there are less Pd active sites [31]. Another drawback of Pd-Ag membranes is the formation of H_2 bubbles on the grain surface at high temperatures (above 450 °C), independent of the fabrication method [34]. Other Pd alloys that have been explored contain copper, ruthenium, gold, yttrium, and nickel. A summary of the

advantages and disadvantages of Pd alloys is reported in Table 3. Pd-Cu alloys are also well-investigated membranes, because of their chemical and thermal stability. Cu has been shown to reduce the temperature where the membrane is subjected to hydrogen embrittlement [35,36]. Jia et al. investigated the behavior at high temperatures and found that the H_2 flux permeation started to decrease after reaching 650 °C [37]. However, reversible loss of H_2 permeation and selectivity towards H_2S were reported by Acha et al. [38]. Gold is also a well-known alloying element with Pd because it enhances hydrogen permeability over pure palladium. Dalla Fontana et al. evaluated the influence of CO, CO_2, and H_2S on a supported Pd-Au membrane, reporting a nearly complete resistance to CO_2, but higher poisoning from CO and H_2S. In the presence of CO, the membrane showed a loss of 89% of H_2 permeance, recovered after 1 hour in the presence of only H_2 at process temperature (400 °C). In the presence of H_2S, they reported a loss of 34% of the original permeance, which could be recovered only by increasing the process temperature to 500 °C for 12 h [39]. Pd-Y is the alloy that guarantees the highest permeability, but it has difficulties in realization, and corrosion problems limit its adoption. Sensitivity to hydrocarbons and carbon monoxide have also been reported [40]. Ruthenium is indicated for low-temperature application compared to other alloys (below 200 °C) [41] and provides a resistance to H_2S poisoning, as reported by [42]. On the other hand, Pd-Ru membranes showed a reduction in H_2 selectivity at 550 °C and bubble formation on grain surface deteriorating the membrane [43]. Omidifar et al. [44] fabricated a 2 µm thick Pd82-Ni18 membrane via electroless-plating (ELP) to reduce cost. When they tested the permeance of the membrane in pure H_2 and with other contaminants, they showed an infinite selectivity towards N_2, reduced permeance with pure H_2 compared to other Pd-Ni membranes with higher Pd concentration, and a reduction of around 50% in permeance in the presence of contaminants like CO and CO_2. The stability test reported no changes in H_2 during the 150 h of the test. The authors conducted a cost analysis, demonstrating that the Pd-Ni alloy had a 38% lower specific cost compared to a pure Pd membrane.

Table 3. Advantages and disadvantages of binary Palladium alloys.

Element	Advantages	Disadvantages	Ref.
Silver (Ag)	• Less expensive • Commercially adopted • Less sensitive to hydrogen embrittlement • Increased Hydrogen permeability	• Sensible to CO poisoning • Sensible to H_2S poisoning • Low durability	[25,31,34,35]
Copper (Cu)	• Higher mechanical stability and durability • Resistance to CO poisoning • Resistance to C_3H_6 poisoning • Resistance at high temperatures (until 650 °C) • Higher permeability than Pd	• Sensible to H_2S poisoning	[25,35–38,45]
Gold (Au)	• Higher permeability than Pd • Resistance to CO_2 poisoning	• Sensible to CO poisoning • Sensible to H_2S poisoning	[37,39]
Yttrium (Y)	• Highest H_2 permeability	• Realization difficulties • Sensible to CO poisoning • Corrosion problems in oxidative activation	[25,40,46]
Ruthenium (Ru)	• Low temperature permeation (below 200 °C) • Good thermal stability • Mechanical properties • Resistance to H_2S poisoning	• Hydrogen selectivity reduced with the temperature above 550 °C; • Bubble formation on grain surface at high temperatures.	[41–43]
Nickel (Ni)	• Reduced cost than pure Pd • Stability	• Reduced permeation than pure Pd • Sensible to CO poisoning • Sensible to CO_2 poisoning	[44]

Ternary Alloys

Following the recent coating techniques, various Pd-based ternary alloys were investigated. Bosko et al. [21] published a review on the performance of Pd-Ag-Au, Pd-Cu-Au, and Pd-Cu-Ag supported membranes. De Noojer et al. [47] tested the influence of H_2S on various Pd-Ag-Au membranes, demonstrating that increasing the Au percentage does not affect the recovery of the membrane from H_2S contamination. In order to reduce membrane costs, ternary alloys, including nickel, were tested. Escalante et al. [48] tested four ELP Pd-Ni-Au membranes with nickel percentages ranging from 29 to 54%, showing nearly infinite selective stability to N_2 and good thermal stability after hydrogenation and dehydrogenation cycles at different temperatures. As expected, palladium concentration had the strongest influence on permeability. Indium was tested as an alloying element to modify lattice parameters, resulting in increased permeation properties. Chen et al. [49] prepared two Pd-Ru-In membranes via ELP with In concentration of 1 and 2%, respectively. Indium positively affects H_2 permeation by doubling and increasing by 50% the H_2 permeability compared to Pd-Ru membranes at 350 and 500 °C, respectively.

3.2. Membrane Types

Equation (7) links the H_2 flux that crosses the membrane to the membrane thickness, showing their inverse proportionality; the thicker the membrane, the higher the H_2 permeating flux. At the same time, the increasing cost of palladium over the last 10 years, reported in Figure 4, drove researchers to investigate various fabrication methods to reduce the thickness of the membranes. Pd-based membranes are categorized into two main types: self-supported and supported, based on whether a porous substrate is used to support thick Pd layers. Figure 5 illustrates this classification of Pd membrane types.

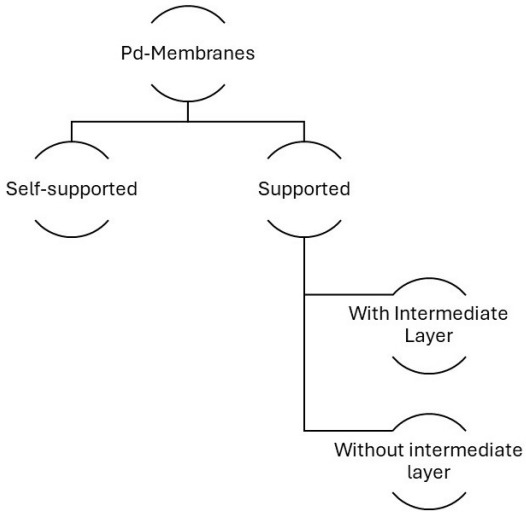

Figure 5. Pd-based membrane configurations.

3.2.1. Self-Supported Membranes

Self-supported Pd-based membranes were typically fabricated through cold rolling, but electroless plating (ELP) was also adopted to achieve a defect-free and mechanically stable 25 µm thick membrane [50]. Currently, research on self-supported membranes is mostly focused to the nuclear sector, more specifically in tritium breeding, a technology adopted for recycling tritium after the deuterium–tritium (D-T) fusion reaction, where the product is a stream of helium and tritium. Wang et al. [51] tested a cold-worked 80 µm $Pd_{92}Y_8$ self-supported membrane for H_2 permeation in H_2/He streams. The membrane, tested with H_2 concentration of 0.1% mol and 0.33% mol, exhibited a permeability of 3.43×10^{-8} mol·m^{-1}·s^{-1}·Pa$^{-0.5}$ at 400 °C. The tests were conducted with variable flow rates (from 7 to 21 standard liter per minute, SLM) and the H_2 recovery showed a decrease with increasing flow rate (from 97.74% to 95%) at 21 SLM with 0.33% mol of H_2 in the

mixture. Combining the properties of Pd-Y and Pd-Ag alloys, Fuerst et al. [52] tested a 76 µm self-supported Pd-Ag membrane in a mixture of deuterium (3.95%) and helium in various combinations of feed pressure and temperature, with permeate pressure of 1 Pa, observing that the permeation values were lower than the values reported in the literature both in pure deuterium and in the mixed gas test. Jazani et al. [53] tested a $Pd_{82}Ag_{15}Y_3$ alloy following the condition $y + 3x \leq 24$ for $Pd_{100-x-y}Ag_yY_x$ [54]. They fabricated a 38 µm thick self-supported membrane by cold rolling and evaluated the performances at 400 °C and pressures ranging from 1.0 to 3.0 bar. The permeation tests showed a better fit, with an n-value of 0.9, attributed to the presence of Ag and Y. The test achieved a permeability of 1.95×10^{-8} mol·m^{-1}·s^{-1}·Pa$^{-0.5}$, which is higher than Pd-Ag membranes and lower than membranes with higher Y content, as reported in the literature. They also tested the performance with different gas mixtures, H_2 and N_2, CO_2, CH_4, and CO, reporting decreases in H_2 permeation in the following order: CO > CO_2 > CH_4 > N_2. The highest reduction in H_2 flux was observed in the test with 40% CO.

3.2.2. Supported Membranes

As an alternative to self-supported membranes, in the last two decades, researchers have focused on reducing membrane thickness to improve hydrogen permeability and reduce costs. Thicker Pd layers require a porous substrate as support for mechanical and thermal stresses. The major investigated supports are metallic or ceramic ones, in particular, porous steel support (PSS) and alumina (Al_2O_3), both in α and γ structures [55,56].

Stainless steel supports offer suitable thermal expansion coefficients for industrial devices but present challenges in preparing ultra-thin H_2 selective films due to high surface roughness and large pores. In recent years, various characteristics of Pd-PSS membranes were tested. Chen et al. [57,58] evaluated the impact of vacuum operation on a 7 µm thick Pd membrane deposited on a PSS substrate modified with α-Al_2O_3 particles. In all their tests of H_2 permeation alone and with other gases (N_2, CO, CO_2), they observed a positive influence of vacuum operation despite the same pressure gradient and the presence of contaminants; the higher the degree of vacuum, the greater the permeated flow rate of H_2. However, the improvement in vacuum decreased with increasing temperatures. Tosto et al. [59] evaluated the effects of concentration polarization effect by N_2 and inhibition effect by CO in three membranes prepared by Electroless Pore-Plating (ELP-PP) and ELP on PSS supports. The lowest concentration polarization and inhibition coefficients were found in the ELP-PP membrane without intermediate layers. PSS supports were also adopted by Peters et al. [34] to evaluate the formation of H_2 bubbles on grain boundaries of the surface of Pd-Ag membranes.

Ceramic supports facilitate the preparation of ultra-thin Pd layers due to lower roughness and controlled pore distribution, but they face challenges regarding thermal resistance and device fitting. Studies on the concentration polarization and competitive adsorption were conducted by Yue et al. [60] on Pd-Al_2O_3-supported membrane fabricated with ELP. Magnone et al. [61] tested the effect of the ELP temperature on the H_2 permeation with a Pd-Al_2O_3-supported membrane, demonstrating that higher ELP temperature produced higher H_2 molar flow rate. This relationship was validated by the thicker Pd layer obtained with increasing process temperature.

In addition to PSS and Al_2O_3 supports, the durability of Pd-supported membranes on tantalium support was investigated by Park et al. [62], highlighting the connection between loss of permeation and temperature; higher temperature correlated with faster reduction of H_2 permeated over time. Tests on Pd-Cu and pure Pd on Ta support membranes were performed [63], demonstrating higher stability (losing only the 50% of the H_2 permeated in 6 h) instead of lower permeability compared to the pure Pd membrane. Yttrium-stabilized Zirconia (YSZ) was investigated as a support under a Pd-Au ELP-fabricated membrane [64]. The authors tested the effect on H_2 permeation with a binary mixture of 50% H_2 and 50% CO with different Au percentages and showed that the alloy with 41% of Au exhibited

no degradation in the presence of CO through the entire test period. A summary of the characteristics of the membranes reviewed above is provided in Table 4.

Table 4. Membrane characteristic of some of the recent works regarding self-supported and supported Pd membranes.

Membrane	Preparation Method	δ_{Pd} [µm]	T [°C]	ΔP [kPa]	H_2 Permeability/ Permeance	$\alpha_{H2/N2}$	Ref.
Pd-Y	Cold-Rolling	80	400	25–300	3.43×10^{-8} (1)	N. D.	[51]
Pd-Ag	Cold-Rolling	76.2	400	≈90	$\approx 8 \times 10^{-9}$ (1)	N.D.	[52]
Pd-Ag-Y	Cold-Rolling	38	400	200	1.95×10^{-8} (1)	∞	[53]
Pd/γ-Al_2O_3	ELP	8.8	350	100	$\approx 4 \times 10^{-6}$ (2)	3.45	[55]
Pd-Au/α-Al_2O_3	ELP	8	400	50	3.87×10^{-3} (2)	500	[56]
Pd/Modified-PSS	ELP	7–8.53	320–380	202.6	$1.47–2.07 \times 10^{-6}$ (2)	92–∞	[57,58]
Pd/PSS	ELP-PP	20	395	200	$\approx 2.5 \times 10^{-4}$ (2)	≥1000	[59]
Pd-Ag/PSS	MS	10	450	400	3.4×10^{-8} (1)	39,000	[34]
Pd/Al_2O_3	ELP	5	350	30–100	4.9×10^{-9} (1)	7935–37,640	[60]
Pd/Ta	ELP	1	450	250	$5.9–12.2 \times 10^{-8}$ (1)	N.D.	[62]

(1) Permeability in $mol \cdot m^{-1} \cdot s^{-1} \cdot Pa^{-0.5}$; (2) Permeance in $mol \cdot m^{-2} \cdot s^{-1} \cdot Pa^{-0.5}$.

3.2.3. Intermediate Layers

To overcome the limitations of metallic supports, researchers are investigating the adoption of ceramic intermediate layers. These layers should possess a thermal expansion coefficient that aligns between the metal support and the Pd-based membrane [65]. One of the most promising intermediate supports is cerium oxide (CeO_2) for Pd-based membranes deposed on PSS [65]. Salomè Macedo et al. [66] tested three different particle sizes of CeO_2 (0.1, 3.4, and >10 µm) as an intermediate layer on a Pd-based membrane on AISI 316L SS support with deposition of palladium by ELP-PP. The medium particle size (3.4 µm) that resulted in a Pd layer thickness of 6.3 µm exhibited the highest H_2 permeability (3.19×10^{-9} $mol \cdot m^{-1} \cdot s^{-1} \cdot Pa^{-0.5}$) and high H_2 selectivity in a test conducted with N_2. Martinez Diaz et al. [67–69] tested the adoption of various types of CeO_2 as intermediate layers in Pd-PSS membranes fabricated by ELP-PP, including raw, Pd-doped, and mesoporous ceria (pore size between 10 and 12 nm) as an intermediate layer for a resulting 10 µm thick Pd membrane and different flux directions. The testing configurations, determined by the sequence in which the feed gas encountered them, is referred to as either IN-OUT or OUT-IN (Figure 6). In the IN-OUT configuration, the feed gas initially interacts with the PSS layer, followed by the Pd-based membrane, a configuration typically adopted in self-supported membranes. Conversely, in the OUT-IN configuration, the feed gas first comes into contact with the Pd-based layer and subsequently the PSS substrate. The permeation tests resulted in higher H_2 permeability with the mesoporous CeO_2 (1.03×10^{-8} $mol \cdot m^{-1} \cdot s^{-1} \cdot Pa^{-0.5}$) than other tests, an infinite selectivity towards N_2 (higher than 24,000), and an assessment of the thermal and mechanical stability of the new membranes. Graphite as intermediate layers was also tested [70], showing an ideal selectivity towards N_2 and a good mechanical stability in the two configurations, OUT-IN and IN-OUT (see Figure 6). Other intermediate layers adopted on PSS substrates are zeolites, like NaY and silicoaluminophosphate zeolite (SAPO-34) [71,72]. The zeolites were deposited by vacuum-assisted seeding and secondary growth, and the Pd-based layer was obtained by ELP. In the two series of experiments, the authors reached a H_2 permeance of 3.81×10^{-4} and 2.47×10^{-4} $mol \cdot m^{-2} \cdot s^{-1} \cdot Pa^{-0.5}$, respectively, a selectivity towards N_2 of 736 and 866, and also a proof of their stability in tests of 130 and 260 h at 450 °C. Sanz-Villanueva et al. [73] used Pd-doped Santa Barbara Amorphous silica (SBA-15), which is widely used as support for catalysts, as an intermediate layer on a PSS support with the Pd layer deposited through ELP-PP. They assessed the positive influence of pre-activating SBA-15 with Pd nuclei on H_2 permeance, on the reduction of the Pd-based layer, and on the mechanical and thermal stability.

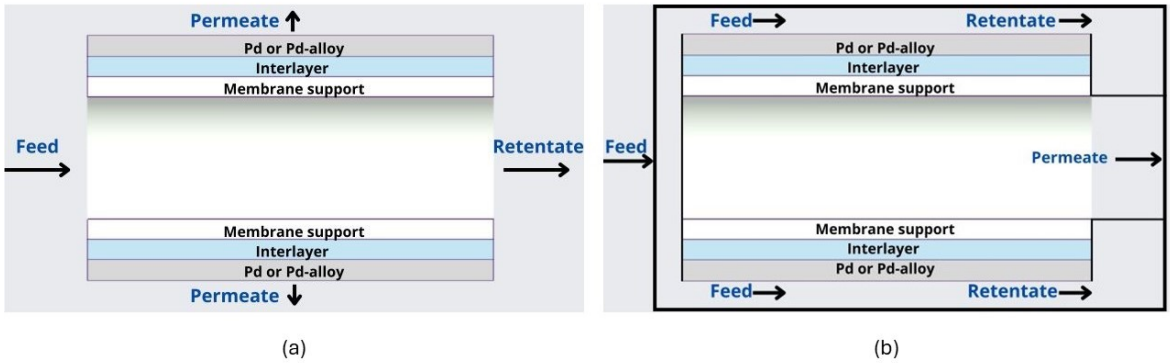

Figure 6. In-Out (**a**) and Out-In (**b**) configuration for supported membrane with intermediate layer.

The impact of the absence of an intermediate layer was also investigated by Iulianelli et al. [56] using a Pd-Au/Al_2O_3 supported membrane, demonstrating that the presence of the intermediate layer did not affect the activation energy but increased the membrane resistance to thermal cycles and degradation. De Moura Silva et al. [74] analyzed the effect of adding a graphene oxide (GO) layer on a Pd/Al_2O_3-supported membrane on H_2 permeation and selectivity towards N_2 and reported a significant increase in membrane selectivity. Zeolite-like materials, such as Nantronite, were tested as an intermediate layer on Al_2O_3-supported membranes to avoid costs connected to the adoption of ultra- or nano-filtering ceramic substrates. Huang et al. [75] analyzed the permeation and the stability of Nantronite 15-A as an intermediate layer for Pd/Al_2O_3 membrane and found an increase in H_2 flux and selectivity after 192 h of testing at 450 °C and a pressure gradient of 1 bar.

Another support investigated in recent years is niobium (Nb) and its alloys. In these supported membranes, an intermediate layer is required because of the inter-diffusion of Pd into Nb at high temperatures. Graphene used as intermediate layer for Pd/Nb membranes [76] was found to be inefficient because of cracking, following the diffusion of Pd into the support. Liang et al. [77] tested the adoption of a hafnium nitride (HfN) layer to inhibit the inter-diffusion of the Pd into the $Nb_{30}Ti_{35}CO_{35}$ support. The membrane was prepared by magnetron sputtering (MS) with a resulting Pd-based layer of 1 µm, and decreases in H_2 were detected only at high temperatures (above 550 °C). A synthesis of experiments with intermediate layers in Pd-supported membranes is reported in Table 5.

Table 5. Recent works adopting intermediate layers on supported Pd membranes.

Membrane	Preparation Method	δ_{Pd} [µm]	T [°C]	ΔP [kPa]	H_2 Permeance/ Permeability	$\alpha_{H2/N2}$	Ref.
Pd/CeO_2/PSS	ELP-PP	10	400	25–300	5.98×10^{-4} (1)	≥10,000	[66]
Pd/CeO_2/PSS	ELP-PP	15.4	400	100–200	5.37×10^{-4} (1)	≥10,000	[67]
Pd/Doped-CeO_2/PSS	ELP-PP	9.1	350–450	100–200	$4.46–6.39 \times 10^{-4}$ (1)	≥10,000	[68]
Pd/Mesoporous-CeO_2/PSS	ELP-PP	10	400	100–200	1.03×10^{-3} (1)	≥24,000	[69]
Pd/Graphite/PSS	ELP-PP	17	400	100	4.01×10^{-4} (1)	≥10,000	[70]
Pd/NaY/PSS	ELP	7	450	100	6.2×10^{-4} (1)	736	[71]
Pd/SAPO-34/PSS	ELP	9	450	100	7.1×10^{-7} (2)	866	[72]
Pd/Doped-SBA-15/PSS	ELP-PP	7.1	400	50–250	3.81×10^{-4} (1)	≥2500	[73]
Pd/GO/Al_2O_3	ELP	0.91	450	100	2.4×10^{-6} (2)	∞	[74]
Pd/NA-15A/Al_2O_3	ELP	2	450	100	≈3.05×10^{-3} (1)	≈3500	[75]
Pd/G/Nb	MS	0.1	450	500	1.83×10^{-9} (3)	N.D	[76]
Pd/HfN/Nb_{30} Ti_{35} CO_{35}	MS	1	250–400	600	2.65×10^{-8} (3)	N.D.	[77]

(1) Permeance in mol·m^{-2}·s^{-1}·Pa$^{-0.5}$; (2) Permeance in mol·m^{-2}·s^{-1}·Pa^{-1};(3) Permeability in mol·m^{-1}·s^{-1}·Pa$^{-0.5}$.

4. Conclusions

In the last few years, there has been a focus in research on the development of new palladium (Pd) alloys to address the limitations observed in commercially available membranes used for hydrogen separation. Notably, considerable attention has been given to

Pd-Au binary and various ternary alloys due to their potential to improve permeability and enhance resistance against poisoning species. Among membrane types, supported membranes have emerged as the most extensively studied. On the other hand, self-supported membranes have found their applications in the nuclear field, where they can be used to separate low-pressure hydrogen isotopes from helium streams in tritium breeding. Efforts to enhance the stability and durability of supported membranes have led researchers to investigate the integration of intermediate layers. These layers play a crucial role in optimizing the membrane's performance under various operating conditions. For the future, there is a growing emphasis on reducing energy consumption associated with hydrogen separation processes. Most of the membranes reviewed in this article belong to laboratory-scale applications. The development of pre-pilot [78] and pilot plants for hydrogen permeation is a pivotal step towards validating and scaling up these membrane technologies for industrial applications. These initiatives are expected to pave the way for the broader adoption of hydrogen separation membranes across various industrial sectors, such as e-fuel production.

Author Contributions: Conceptualization, N.C. and F.Z.; methodology, F.Z. and G.D.Z.; software, G.D.Z.; validation, N.C., F.Z. and L.F.; formal analysis, C.F.; investigation, G.D.Z., C.F. and F.Z.; resources, G.D.Z. and C.F. ; data curation, G.D.Z., C.F. and F.Z.; writing—original draft preparation, G.D.Z. and C.F.; writing—review and editing, N.C., F.Z. and L.F.; visualization, G.D.Z. and C.F.; supervision, N.C. and F.Z.; project administration, N.C. and F.Z. All authors have read and agreed to the published version of the manuscript.

Funding: Work funded by the Italian Ministry of the Environment and Energy Security, program agreement MiTE-ENEA PNRR-Hydrogen Research-Mission M2-C4 - Investment 3.5: Research and development on hydrogen.

Data Availability Statement: No new data have been created.

Acknowledgments: Maria A. Cerone is gratefully acknowledged for the language revision.

Conflicts of Interest: The authors declare no conflicts of interest.

Abbreviations

The following abbreviations are used in this manuscript:

WMO	World Meteorological Organization
GHG	Greenhouse Gas
CCUS	Carbon Capture Utilization and Storage
PEMFC	Proton Exchange Membrane Fuel Cell
PSA	Pressure Swing Adsorption
BCC	Body-Centered Cubic
FCC	Face-Centered Cubic
PSS	Porous Steel Support
ELP	Electroless Plating
ELP-PP	Electroless Pore-Plating
MS	Magnetron Sputtering

References

1. World Meterological Organization. WMO Confirms 2023 Smashes Global Temperature Record. 2023. Available online: https://wmo.int/news/media-centre/wmo-confirms-2023-smashes-global-temperature-record (accessed on 26 April 2024).
2. Farias, C.B.B.; Barreiros, R.C.S.; da Silva, M.F.; Casazza, A.A.; Converti, A.; Sarubbo, L.A. Use of Hydrogen as Fuel: A Trend of the 21st Century. *Energies* **2022**, *15*, 311. [CrossRef]
3. Osselin, F.; Soulaine, C.; Fauguerolles, C.; Gaucher, E.; Scaillet, B.; Pichavant, M. Orange hydrogen is the new green. *Nat. Geosci.* **2022**, *15*, 765–769. [CrossRef]
4. Arcos, J.M.M.; Santos, D.M.F. The Hydrogen Color Spectrum: Techno-Economic Analysis of the Available Technologies for Hydrogen Production. *Gases* **2023**, *3*, 25–46. [CrossRef]
5. Yao, D.; Zhang, Y.; Williams, P.T.; Yang, H.; Chen, H. Co-production of hydrogen and carbon nanotubes from real-world waste plastics: Influence of catalyst composition and operational parameters. *Appl. Catal. Environ.* **2018**, *221*, 584–597. [CrossRef]

6. IEA. Global Hydrogen Review 2023. 2023. Available online: https://www.iea.org/reports/global-hydrogen-review-2023 (accessed on 26 April 2024).
7. Shchegolkov, A.V.; Shchegolkov, A.V.; Zemtsova, N.V.; Stanishevskiy, Y.M.; Vetcher, A.A. Recent Advantages on Waste Management in Hydrogen Industry. *Polymers* **2022**, *14*, 4992. [CrossRef] [PubMed]
8. Wan, C.; Li, R.; Wang, J.; Cheng, D.g.; Chen, F.; Xu, L.; Gao, M.; Kang, Y.; Eguchi, M.; Yamauchi, Y. Silica Confinement for Stable and Magnetic Co-Cu Alloy Nanoparticles in Nitrogen-Doped Carbon for Enhanced Hydrogen Evolution. *Angew. Chem. Int. Ed.* **2024**, *63*, e202404505. [CrossRef] [PubMed]
9. Tang, S.; Zhang, Z.; Xu, L.; Qin, H.; Dong, J.; Lv, Q.; Han, J.; Song, F. Ultrafine nickel-rhodium nanoparticles anchored on two-dimensional vanadium carbide for high performance hydrous hydrazine decomposition at mild conditions. *J. Colloid Interface Sci.* **2024**, *669*, 228–235. [CrossRef] [PubMed]
10. Das, S.K.; Reis, A.; Berry, K. Experimental evaluation of CO poisoning on the performance of a high temperature proton exchange membrane fuel cell. *J. Power Sources* **2009**, *193*, 691–698. [CrossRef]
11. *ISO 14687:2019*; Hydrogen Fuel Quality—Product Specification. International Standard: Geneva, Switzerland, 2019. Available online: https://www.iso.org/standard/69539.html (accessed on 26 April 2024).
12. Du, Z.; Liu, C.; Zhai, J.; Guo, X.; Xiong, Y.; Su, W.; He, G. A Review of Hydrogen Purification Technologies for Fuel Cell Vehicles. *Catalysts* **2021**, *11*, 393. [CrossRef]
13. SIRCAR, S.; GOLDEN, T.C. Purification of Hydrogen by Pressure Swing Adsorption. *Sep. Sci. Technol.* **2000**, *35*, 667–687. [CrossRef]
14. Bang, G.; Moon, D.K.; Kang, J.H.; Han, Y.J.; Kim, K.M.; Lee, C.H. High-purity hydrogen production via a water-gas-shift reaction in a palladium-copper catalytic membrane reactor integrated with pressure swing adsorption. *Chem. Eng. J.* **2021**, *411*, 128473. [CrossRef]
15. Shaposhnik, V.A. Prospects of membrane catalysis in hydrogen energetics. Mini review. *Condens. Matter Interphases* **2024**, *26*, 37–44. [CrossRef]
16. Stenina, I.; Yaroslavtsev, A. Modern Technologies of Hydrogen Production. *Processes* **2023**, *11*, 56. [CrossRef]
17. Jokar, S.; Farokhnia, A.; Tavakolian, M.; Pejman, M.; Parvasi, P.; Javanmardi, J.; Zare, F.; Gonçalves, M.C.; Basile, A. The recent areas of applicability of palladium based membrane technologies for hydrogen production from methane and natural gas: A review. *Int. J. Hydrogen Energy* **2023**, *48*, 6451–6476. [CrossRef]
18. Habib, M.A.; Haque, M.A.; Harale, A.; Paglieri, S.; Alrashed, F.S.; Al-Sayoud, A.; Nemitallah, M.A.; Hossain, S.; Abuelyamen, A.; Mokheimer, E.M.; et al. Palladium-alloy membrane reactors for fuel reforming and hydrogen production: Hydrogen Production Modeling. *Case Stud. Therm. Eng.* **2023**, *49*, 103359. [CrossRef]
19. Chen, W.H.; Chen, C.Y. Water gas shift reaction for hydrogen production and carbon dioxide capture: A review. *Appl. Energy* **2020**, *258*, 114078. [CrossRef]
20. Suzuki, A.; Yukawa, H. A Review for Consistent Analysis of Hydrogen Permeability through Dense Metallic Membranes. *Membranes* **2020**, *10*, 120. [CrossRef]
21. Bosko, M.L.; Dalla Fontana, A.; Tarditi, A.; Cornaglia, L. Advances in hydrogen selective membranes based on palladium ternary alloys. *Int. J. Hydrogen Energy* **2021**, *46*, 15572–15594. [CrossRef]
22. Girotto, C.P.; Nippes, R.P.; Macruz, P.D.; Gomes, A.D.; de Souza, M.; Rodriguez, M.T. Effect of physicochemical properties on the performance of palladium-based composite membranes: A review. *J. Mater. Res.* **2023**, *38*, 4868–4891. [CrossRef]
23. Shere, L.; Hill, A.K.; Mays, T.J.; Lawless, R.; Brown, R.; Perera, S.P. The next generation of low tritium hydrogen isotope separation technologies for future fusion power plants. *Int. J. Hydrogen Energy* **2024**, *55*, 319–338. [CrossRef]
24. Graham, T. On the absorption and dialytic separation of gases by colloid septa. *J. Frankl. Inst.* **1867**, *83*, 39–41. [CrossRef]
25. Al-Mufachi, N.; Rees, N.; Steinberger-Wilkens, R. Hydrogen selective membranes: A review of palladium-based dense metal membranes. *Renew. Sustain. Energy Rev.* **2015**, *47*, 540–551. [CrossRef]
26. Yun, S.; Ted Oyama, S. Correlations in palladium membranes for hydrogen separation: A review. *J. Membr. Sci.* **2011**, *375*, 28–45. [CrossRef]
27. Rahimpour, M.; Samimi, F.; Babapoor, A.; Tohidian, T.; Mohebi, S. Palladium membranes applications in reaction systems for hydrogen separation and purification: A review. *Chem. Eng. Process. Process. Intensif.* **2017**, *121*, 24–49. [CrossRef]
28. Morreale, B.D. The Influence of H2S on Palladium and Palladium-Copper Alloy mMembranes. Ph.D. Thesis, University of Pittsburgh, Pittsburgh, PA, USA, 2007.
29. Dolan, M. Non-Pd BCC alloy membranes for industrial hydrogen separation. *J. Membr. Sci.* **2010**, *362*, 12–28. [CrossRef]
30. Cardoso, S.P.; Azenha, I.S.; Lin, Z.; Portugal, I.; Rodrigues, A.E.; Silva, C.M Inorganic Membranes for Hydrogen Separation. *Sep. Purif. Rev.* **2018**, *47*, 229–266. [CrossRef]
31. Easa, J.; Yan, C.; Schneider, W.F.; O'Brien, C.P. CO and C_3H_6 poisoning of hydrogen permeation across $Pd_{77}Ag_{23}$ alloy membranes: A comparative study with pure palladium. *Chem. Eng. J.* **2022**, *430*, 133080. [CrossRef]
32. Gabitto, J.; Tsouris, C. Modeling sulfur poisoning of palladium membranes used for hydrogen separation. *Int. J. Chem. Eng.* **2019**, *2019*, 9825280. [CrossRef]
33. Macrotrends. 2024. Available online: https://www.macrotrends.net/2542/palladium-prices-historical-chart-data (accessed on 26 April 2024).

34. Peters, T.; Carvalho, P.; Stange, M.; Bredesen, R. Formation of hydrogen bubbles in Pd-Ag membranes during H_2 permeation. *Int. J. Hydrogen Energy* **2020**, *45*, 7488–7496. [CrossRef]
35. Peters, T.; Kaleta, T.; Stange, M.; Bredesen, R. Hydrogen transport through a selection of thin Pd-alloy membranes: Membrane stability, H2S inhibition, and flux recovery in hydrogen and simulated WGS mixtures. *Catal. Today* **2012**, *193*, 8–19. [CrossRef]
36. Pati, S.; Ashok, J.; Dewangan, N.; Chen, T.; Kawi, S. Ultra-thin (1 μm) Pd–Cu membrane reactor for coupling CO2 hydrogenation and propane dehydrogenation applications. *J. Membr. Sci.* **2020**, *595*, 117496. [CrossRef]
37. Jia, H.; Wu, P.; Zeng, G.; Salas-Colera, E.; Serrano, A.; Castro, G.R.; Xu, H.; Sun, C.; Goldbach, A. High-temperature stability of Pd alloy membranes containing Cu and Au. *J. Membr. Sci.* **2017**, *544*, 151–160. [CrossRef]
38. Acha, E.; van Delft, Y.; Cambra, J.; Arias, P. Thin PdCu membrane for hydrogen purification from in-situ produced methane reforming complex mixtures containing H_2S. *Chem. Eng. Sci.* **2018**, *176*, 429–438. [CrossRef]
39. Dalla Fontana, A.; Sirini, N.; Cornaglia, L.M.; Tarditi, A.M. Hydrogen permeation and surface properties of PdAu and PdAgAu membranes in the presence of CO, CO_2 and H_2S. *J. Membr. Sci.* **2018**, *563*, 351–359. [CrossRef]
40. Conde, J.J.; Maroño, M.; Sánchez-Hervás, J.M. Pd-Based Membranes for Hydrogen Separation: Review of Alloying Elements and Their Influence on Membrane Properties. *Sep. Purif. Rev.* **2017**, *46*, 152–177. [CrossRef]
41. Lee, S.M.; Xu, N.; Kim, S.S.; Li, A.; Grace, J.R.; Lim, C.J.; Boyd, T.; Ryi, S.K.; Susdorf, A.; Schaadt, A. Palladium/ruthenium composite membrane for hydrogen separation from the off-gas of solar cell production via chemical vapor deposition. *J. Membr. Sci.* **2017**, *541*, 1–8. [CrossRef]
42. Yin, Z.; Yang, Z.; Tong, Y.; Du, M.; Mi, J.; Yu, Q.; Li, S. Improved sulfur tolerance of Pd–Ru membranes: Influence of H_2S concentration and exposure time on the hydrogen flux. *Int. J. Hydrogen Energy* **2023**, *48*, 38335–38343. [CrossRef]
43. Liu, J.; Bellini, S.; de Nooijer, N.C.; Sun, Y.; Pacheco Tanaka, D.A.; Tang, C.; Li, H.; Gallucci, F.; Caravella, A. Hydrogen permeation and stability in ultra-thin PdRu supported membranes. *Int. J. Hydrogen Energy* **2020**, *45*, 7455–7467. [CrossRef]
44. Omidifar, M.; Akbar Babaluo, A.; Jamshidi, S. H_2 permeance and surface characterization of a thin (2 μm) Pd-Ni composite membrane prepared by electroless plating. *Chem. Eng. Sci.* **2024**, *283*, 119370. [CrossRef]
45. O'Brien, C.P.; Lee, I.C. The interaction of CO with PdCu hydrogen separation membranes: An operando infrared spectroscopy study. *Catal. Today* **2019**, *336*, 216–222. [CrossRef]
46. Peng, L.; Rao, Y.; Luo, L.; Chen, C. The poisoning of Pd–Y alloy membranes by carbon monoxide. *J. Alloys Compd.* **2009**, *486*, 74–77. [CrossRef]
47. de Nooijer, N.; Sanchez, J.D.; Melendez, J.; Fernandez, E.; Pacheco Tanaka, D.A.; van Sint Annaland, M.; Gallucci, F. Influence of H2S on the hydrogen flux of thin-film PdAgAu membranes. *Int. J. Hydrogen Energy* **2020**, *45*, 7303–7312. [CrossRef]
48. Escalante, Y.; Tarditi, A.M. Thermally stable membranes based on PdNiAu systems with high nickel content for hydrogen separation. *J. Membr. Sci.* **2023**, *676*, 121581. [CrossRef]
49. Chen, Z.; Yang, Z.; Tong, Y.; Yin, Z.; Li, S. High hydrogen permeability of Pd-Ru-In membranes prepared by electroless co-deposition. *Sep. Purif. Technol.* **2024**, *343*, 127073. [CrossRef]
50. Mukaida, M.; Takahashi, N.; Hisamatsu, K.; Ishitsuka, M.; Hara, S.; Suda, H.; Haraya, K. Preparation for defect-free self-supported Pd membranes by an electroless plating method. *J. Membr. Sci.* **2010**, *365*, 378–381. [CrossRef]
51. Wang, X.; Feng, X.; Yang, L.; An, Y.; Yao, Y.; Chen, K.; Song, J.; Shi, Y.; Chen, C.; Luo, W. Highly efficient and direct recovery of low-pressure hydrogen isotopes from tritium extraction gas by PdY alloy membrane permeator. *Fusion Eng. Des.* **2024**, *202*, 114348. [CrossRef]
52. Fuerst, T.F.; Taylor, C.N.; Shimada, M. Deuterium Permeation Through a Self-Supported Palladium-Silver Membrane in Helium Gas Mixtures. *IEEE Trans. Plasma Sci.* **2024**, 1–5. [CrossRef]
53. Jazani, O.; Bennett, J.; Liguori, S. Effect of temperature, air exposure and gas mixture on Pd82–Ag15–Y3 membrane for hydrogen separation. *Int. J. Hydrogen Energy* **2024**, *51*, 624–636. [CrossRef]
54. Sakamoto, Y.; Chen, F.; Furukawa, M.; Mine, K. The (α + β) hydrogen miscibility gaps in hydrogenated palladium-rich Pd-Y(Gd)-Ag ternary alloys. *J. Less Common Met.* **1990**, *166*, 45–56. [CrossRef]
55. Orakwe, I.; Shehu, H.; Gobina, E. Preparation and characterization of palladium ceramic alumina membrane for hydrogen permeation. *Int. J. Hydrogen Energy* **2019**, *44*, 9914–9921. [CrossRef]
56. Iulianelli, A.; Jansen, J.C.; Esposito, E.; Longo, M.; Dalena, F.; Basile, A. Hydrogen permeation and separation characteristics of a thin Pd-Au/Al_2O_3 membrane: The effect of the intermediate layer absence. *Catal. Today* **2019**, *330*, 32–38. [CrossRef]
57. Chen, W.H.; Lin, S.W.; Chen, C.Y.; Chi, Y.H.; Lin, Y.L. Impact of vacuum operation on hydrogen permeation through a palladium membrane tube. *Int. J. Hydrogen Energy* **2019**, *44*, 14434–14444. [CrossRef]
58. Chen, W.H.; Escalante, J. Influence of vacuum degree on hydrogen permeation through a Pd membrane in different H_2/N_2 gas mixtures. *Renew. Energy* **2020**, *155*, 1245–1263. [CrossRef]
59. Tosto, E.; Martinez-Diaz, D.; Sanz, R.; Azzato, G.; Calles, J.A.; Medrano, J.A.; Fernandez, E.; Pacheco Tanaka, D.A.; Gallucci, F.; Alique, D.; et al. Systematic experimental assessment of concentration polarization and inhibition in Pd-based membranes for hydrogen purification. *Fuel Process. Technol.* **2021**, *213*, 106661. [CrossRef]
60. Yue, L.; Chen, C.; Li, J.; Xiao, C.; Xia, X.; Ran, G.; Fu, X.; Hou, J.; Gong, Y.; Wang, H. Inhibition Effect of CO on Hydrogen Permeation Through a Pd/Al_2O_3 Composite Membrane: A Comprehensive Study on Concentration Polarization and Competitive Adsorption Effect. *Fusion Sci. Technol.* **2020**, *76*, 680–689. [CrossRef]

61. Magnone, E.; Lee, S.H.; Park, J.H. Relationships between electroless plating temperature, Pd film thickness and hydrogen separation performance of Pd-coated Al_2O_3 hollow fibers. *Mater. Lett.* **2020**, *272*, 127811. [CrossRef]
62. Park, Y.; Kwak, Y.; Yu, S.; Badakhsh, A.; Lee, Y.J.; Jeong, H.; Kim, Y.; Sohn, H.; Nam, S.W.; Yoon, C.W.; et al. Degradation mechanism of a Pd/Ta composite membrane: Catalytic surface fouling with inter-diffusion. *J. Alloys Compd.* **2021**, *854*, 157196. [CrossRef]
63. Ryu, S.; Badakhsh, A.; Oh, J.G.; Ham, H.C.; Sohn, H.; Yoon, S.P.; Choi, S.H. Experimental and Numerical Study of Pd/Ta and PdCu/Ta Composites for Thermocatalytic Hydrogen Permeation. *Membranes* **2023**, *13*, 23. [CrossRef]
64. Lundin, S.T.B.; Patki, N.S.; Zhang, Z.; Fuerst, T.F.; Wolden, C.A.; Way, J.D. PdAu/YSZ composite hydrogen separation membranes with enhanced stability in the presence of CO. *J. Membr. Sci.* **2020**, *611*, 118371. [CrossRef]
65. Alique, D.; Martinez-Diaz, D.; Sanz, R.; Calles, J.A. Review of Supported Pd-Based Membranes Preparation by Electroless Plating for Ultra-Pure Hydrogen Production. *Membranes* **2018**, *8*, 5. [CrossRef]
66. Salomé Macedo, M.; Acha Uriarte, N.; Soria, M.; Madeira, L.M.; Calles, J.; Sanz, R.; Alique, D. Effect of ceria particle size as intermediate layer for preparation of composite Pd-membranes by electroless pore-plating onto porous stainless-steel supports. *Sep. Purif. Technol.* **2023**, *327*, 124932. [CrossRef]
67. Martinez-Diaz, D.; Sanz, R.; Calles, J.; Alique, D. H2 permeation increase of electroless pore-plated Pd/PSS membranes with CeO2 intermediate barriers. *Sep. Purif. Technol.* **2019**, *216*, 16–24. [CrossRef]
68. Martinez-Diaz, D.; Alique, D.; Calles, J.; Sanz, R. Pd-thickness reduction in electroless pore-plated membranes by using doped-ceria as interlayer. *Int. J. Hydrogen Energy* **2020**, *45*, 7278–7289. [CrossRef]
69. Martinez-Diaz, D.; Martínez del Monte, D.; García-Rojas, E.; Alique, D.; Calles, J.; Sanz, R. Comprehensive permeation analysis and mechanical resistance of electroless pore-plated Pd-membranes with ordered mesoporous ceria as intermediate layer. *Sep. Purif. Technol.* **2021**, *258*, 118066. [CrossRef]
70. Martinez-Diaz, D.; Sanz, R.; Carrero, A.; Calles, J.A.; Alique, D. Effective H2 Separation through Electroless Pore-Plated Pd Membranes Containing Graphite Lead Barriers. *Membranes* **2020**, *10*, 410. [CrossRef] [PubMed]
71. Kiadehi, A.D.; Taghizadeh, M. Fabrication, characterization, and application of palladium composite membrane on porous stainless steel substrate with NaY zeolite as an intermediate layer for hydrogen purification. *Int. J. Hydrogen Energy* **2019**, *44*, 2889–2904. [CrossRef]
72. Dehghani Kiadehi, A.; Taghizadeh, M.; Rami, M.D. Preparation of Pd/SAPO-34/PSS composite membranes for hydrogen separation: Effect of crystallization time on the zeolite growth on PSS support. *J. Ind. Eng. Chem.* **2020**, *81*, 206–218. [CrossRef]
73. Sanz-Villanueva, D.; Alique, D.; Vizcaíno, A.; Sanz, R.; Calles, J. Pre-activation of SBA-15 intermediate barriers with Pd nuclei to increase thermal and mechanical resistances of pore-plated Pd-membranes. *Int. J. Hydrogen Energy* **2021**, *46*, 20198–20212. [CrossRef]
74. de Moura Silva, C.L.; Ribeiro, S.R.F.L.; Terra, N.M.; Cardoso, V.L.; Reis, M.H.M. Improved hydrogen permeation through thin Pd/Al2O3 composite membranes with graphene oxide as intermediate layer. *Int. J. Hydrogen Energy* **2020**, *45*, 22990–23005. [CrossRef]
75. Huang, Y.; Liu, Q.; Jin, X.; Ding, W.; Hu, X.; Li, H. Coating the porous Al_2O_3 substrate with a natural mineral of Nontronite-15A for fabrication of hydrogen-permeable palladium membranes. *Int. J. Hydrogen Energy* **2020**, *45*, 7412–7422. [CrossRef]
76. Guo, Y.; Guo, Y.; Zou, D.; Pan, Q.; Jiang, C.; Li, Y.; Chen, C. Effect of single atomic layer graphene film on the thermal stability and hydrogen permeation of Pd-coated Nb composite membrane. *Int. J. Hydrogen Energy* **2022**, *47*, 8359–8371. [CrossRef]
77. Liang, X.; Li, X.; Chen, R.; Nagaumi, H.; Guo, J.; Liu, D. Enhancement of hydrogen permeation stability at high temperatures for Pd/Nb30Ti35Co35/Pd composite membranes by HfN intermediate layer. *J. Membr. Sci.* **2022**, *643*, 120062. [CrossRef]
78. Cerone, N.; Zimbardi, F.; Contuzzi, L.; Tosti, S.; Fabbiano, L.; Zito, G.D.; Carnevale, M.O.; Valerio, V. Pre-pilot scale study of hydrogen production from biomass syngas via water-gas shift in Pd–Ag catalytic membrane reactor and dedicated hydrogen permeation unit. *Int. J. Hydrogen Energy* 2024, *in press*. [CrossRef]